

Selection and Stability Validation of Reference Gene Candidates for Transcriptional Analysis in *Rousettus Aegyptiacus*

Virginia Friedrichs

Friedrich-Loeffler-Institut, Greifswald-Insel Riems

Anne Balkema-Buschmann

Friedrich-Loeffler-Institut, Greifswald-Insel Riems

Anca Dorhoi

Friedrich-Loeffler-Institut, Greifswald-Insel Riems

Gang Pei (✉ Gang.Pei@fli.de)

Friedrich-Loeffler-Institut, Greifswald-Insel Riems

Research Article

Keywords: Selection, stability, validation, gene candidates, analysis, mammals, body temperature, species

Posted Date: June 16th, 2021

DOI: <https://doi.org/10.21203/rs.3.rs-604945/v1>

License:  This work is licensed under a Creative Commons Attribution 4.0 International License.

[Read Full License](#)

Abstract

Bats are the only mammals capable of powered flight and their body temperature can reach up to 42°C during flight. Additionally, bats display robust type I IFN interferon (IFN-I) responses and some species constitutively express IFN- α . Reference genes with stable expression under temperature oscillations and IFN-I release are therefore critical for normalization of quantitative reverse-transcription polymerase chain reaction (qRT-PCR) data in bats. The expression stability of reference genes in *Rousettus aegyptiacus* remains elusive, although this species is frequently used in the infection research. We selected *ACTB*, *EEF1A1*, *GAPDH* and *PGK1* as candidate reference genes and evaluated their expression stability in various tissues and cells from this model bat species upon IFN-I treatment at 37°C and 40°C by qRT-PCR. We employed two statistical algorithms, BestKeeper and NormFinder, and found that *EEF1A1* exhibited the highest stability under all tested conditions. *ACTB* and *GAPDH* displayed unstable expression at 40°C and upon IFN-I treatment, respectively. By normalizing to *EEF1A1*, we uncovered that *GAPDH* expression was significantly induced by IFN-I in *R. aegyptiacus*. Our study identifies *EEF1A1* as the most suitable reference gene for qRT-PCR studies and unveils the induction of *GAPDH* expression by IFN-I in *R. aegyptiacus*. These findings are pertinent to other bat species and even bear relevance for non-volant mammals that show physiological fluctuations of core body temperature.

Introduction

Bats are increasingly recognized as reservoir hosts of highly-virulent pathogens, such as Filoviruses, Lyssaviruses, Paramyxoviruses and Coronaviruses, including severe acute respiratory syndrome coronavirus 2 (SARS-CoV-2), which causes the current global pandemic¹. Particularly, Egyptian fruit bats, *Rousettus aegyptiacus*, have been identified as putative reservoir hosts of Marburg virus², Kasokero virus³ and Sosuga virus⁴, and were shown to be susceptible to experimental challenge with SARS-CoV-2⁵ and Rift valley fever phlebovirus⁶. These viruses may cause severe diseases with high mortality rates in humans. However, bats show minimal and often even no clinical manifestation upon natural infection. Under experimental conditions, *Rousettus* bats infected with high doses of Ebola⁷, SARS-CoV⁸ or SARS-CoV-2⁵ support transient viral replication and display limited pathology. Several hypotheses could explain the reservoir potential of bats. As the only mammals capable of powered flight, their body temperature can reach 42°C during flight⁹. Hence, 'flight-as-fever' has been postulated as a unique mechanism conferring effective immune defence similar to fever⁶. Further, the black flying fox, *Pteropus alecto*, constitutively expresses IFN- α ¹⁰, and gene loci of type I interferons (IFN-I) in *R. aegyptiacus*, are markedly expanded¹¹, indicating a potential contribution of boosted IFN-I signalling to antiviral immunity in bats. In addition to the enhanced antiviral immunity, bats suppress excessive inflammation which may explain their lack of symptoms during viral infection^{1,12}. For example, *TNF α* expression in *Eptesicus fuscus* cells is abolished upon poly(I:C) stimulation¹³, NLRP3-mediated inflammasome activation is impaired in *P. alecto*¹⁴ and *Myotis davidii*¹², and *R. aegyptiacus* does not upregulate pro-inflammatory genes (*CCL8*, *FAS* and *IL6*) upon Marburg virus infection¹⁵. Enhanced antiviral immunity along with reduced

inflammation likely explains the ability of bats to harbour high-impact pathogens in absence of clinical disease. Confirmation of these findings in distinct bat species as well as elucidation of novel immune mechanisms contributing to the reservoir potential of bats require accurate monitoring of their immune responses.

The knowledge about the exceptional immune system of bats has significantly advanced during the past decade¹⁶. However, experimental tools to systematically investigate bat immune responses, such as species-specific or cross-reactive antibodies, are largely missing¹⁷⁻¹⁹. Accordingly, investigations on host immunity heavily rely on gene transcription profiling by real-time quantitative reverse transcription PCR (qRT-PCR). This method is sensitive, specific, highly reproducible and accurate^{20,21}. A critical step in qRT-PCR setup is represented by the selection of several stable reference genes. The inclusion of such reference genes is crucial for gene expression normalization and subsequent data interpretation. The ideal reference genes should maintain stable expression levels across diverse tissues and cell types as well as under different experimental conditions²². Considering that bats display unique physiological features, notably oscillating metabolic rates and core body temperature depending on flying and roosting phases²³⁻²⁶, the expression stability of reference genes must be evaluated taking these conditions into account. Multiple reference genes, including glyceraldehyde-3-phosphate dehydrogenase (*GAPDH*), actin-beta (*ACTB*), small nuclear ribonucleoprotein Sm D3 (*SNRPD3*) and 18S ribosomal RNA (*18S rRNA*) have been employed in gene expression studies of *P. alecto*, *E. fuscus*, *M. davidii* and other bats^{13,14,27-29}. However, a comprehensive analysis of reference genes, particularly their expression stability under oscillating temperatures, has not been performed in bats, including the model bat *R. aegyptiacus*.

Here, we provide a first in-depth validation of four reference gene candidates, including *ACTB*, *GAPDH*, eukaryotic translation elongation factor 1 alpha 1 (*EEF1A1*) and phosphoglycerate kinase 1 (*PGK1*) for *R. aegyptiacus*. Our findings support *EEF1A1* as the best reference gene for normalization of qRT-PCR data in the Egyptian fruit bat and call for caution when using other candidate genes, i.e. *GAPDH* and *ACTB*, due to their instability under specific conditions.

Material And Methods

Selection of reference gene candidates and design of primer pairs. Reference gene candidates (*ACTB*, *EEF1A1*, *GAPDH* and *PGK1*) for *R. aegyptiacus* gene expression studies were selected based on their utilization in other bat species^{13,14,17}. Primers against these reference genes were designed using the PrimerQuest tool (Integrated DNA Technologies, Inc.). The criteria for primer design were as follows: primer lengths around 17-30 bp, GC content of 40-55%, optimal melting temperature at 62°C, and amplicon lengths within a range of 100-250 bp. Derived primer pairs were evaluated using the OligoAnalyzer tool to exclude primers with hairpin structures and homo- and/or heterodimer formation (Integrated DNA Technologies, Inc.). Primer sequences were also blasted using the NCBI BLAST tool to ensure their specificity for *R. aegyptiacus*. The primer pairs meeting all criteria were selected for further experiments. The characteristics of these primers are shown in Table 4.

Table 4. Summary of selected reference gene candidates.

Gene symbol	Gene name	Gene ID	Primer sequence [5'-3']	Amplicon size [bp]
<i>ACTB</i>	actin beta	107515934	F- GCCTTGGTCGTGGATAATG R- GGGATACTTCAGGGTCAGGATA	193
<i>EEF1A1</i>	eukaryotic translation elongation factor 1 alpha 1	107509282	F- GTATGCCTGGGTCTTGGATAAA R- GCCTGTGATGTGCCTGTAA	162
<i>GAPDH</i>	glyceraldehyde-3-phosphate dehydrogenase	107519804	F- CAAGTTCAAAGGCACAGTCAAG R- TATTCAGCACCAGCATCACC	120
<i>PGK1</i>	phosphoglycerate kinase 1	107503843	F- GATTACCTTGCCTGTTGACTTTG R- GACAGCCTCAGCATACTTCTT	148

Cells, tissues and stimulation experiments. Bat fibroblasts were derived from the lung of a female *R. aegyptiacus* bat from the *R. aegyptiacus* breeding colony at the Friedrich-Loeffler-Institut. Sampling was performed in accordance with current European and National Animal Welfare regulations, after ethical review and approval by the authority of the Federal State of Mecklenburg-Western Pomerania, Germany (file number 7221.3-2-042/17) and the experiments were carried out according to ARRIVE guidelines (<https://arriveguidelines.org>). The lung tissue was dissected into small pieces and digested with trypsin overnight at 4°C. Dissociated cells were seeded in cell culture dishes in DMEM medium (DMEM high glucose medium, 10% fetal bovine serum (FBS), 2 mM glutamine and 100 U/mL of Penicillin-Streptomycin) for 2 h, and only adherent cells were propagated. Confirmation of bat fibroblast identity was carried out by examining fibroblast activation protein (FAP) expression via PCR (data not shown).

Tissue samples from 12 individual bats were obtained from an animal experiment published before⁷⁶. For IFN-I stimulation, bat fibroblasts and human dermal fibroblasts (#C0045C, ThermoFisher Scientific) were incubated with 1000 U/ml universal IFN-I (uIFN) (#11200-1, PBL Assay Science) for 1 h, 2 h and 4 h at either 37°C or 40°C, respectively.

RNA extraction and cDNA synthesis. Cells were lysed in homemade Trizol solution and RNA was extracted as published before⁷⁷. Purified RNA was quantified using NanoDrop 2000c spectrophotometer (#ND-2000c, ThermoFisher Scientific) and 800ng RNA were subsequently utilized for cDNA synthesis with the LunaScript RT SuperMix Kit (#E3010L, New England BioLabs).

qRT-PCR. qRT-PCR reactions were carried out with EvaGreen® Fluorescent DNA stain (# PCR-379, Jena Bioscience), ROX as an internal reference dye (#PCR-351, Jena Bioscience) and GoTaq® Polymerase

(#M3001, Promega) according to manufacturers' instructions. The reaction setup was as follows: 95°C for 2 min; (95°C for 30s, 62°C for 30s, 72°C for 1 min) for 40 cycles; 72°C for 10 min and infinite hold at 4°C. Unless stated otherwise, each qPCR reaction was performed with 100ng cDNA. To minimize pipetting errors, the template was diluted and 5µl were used for each qRT-PCR reaction. Measurements were performed with the QuantStudio™ 6 Flex Real-Time PCR System (#4485691, Applied Biosystems™). Melting curves were performed within the temperature range from 60.16°C to 94.885°C in steps of 0.193°C, respectively.

Establishment of standard curves and examination of amplification efficiency via qRT-PCR. Standard curves of all reference genes in the qRT-PCR reaction were generated with copy numbers from 300,000 to 3 copies in 10-fold dilution steps. To achieve accurate copy numbers, amplicon sizes of each reference gene were used to calculate the specific weight of each amplicon⁷⁸, resulting in 2.12×10^{-19} g for *ACTB*, 1.78×10^{-19} g for *EEF1A1*, 1.32×10^{-19} g for *GAPDH* and 1.62×10^{-19} g for *PGK1*. The amplification efficiency of all primer pairs was subsequently determined with the slope of the standard curve according to the equation $10^{-1/\text{slope}-1}$. The amplification efficiency of favourable primers ranges between 90-110%. Linear dynamic range (LDR) is described as the highest to the lowest quantifiable copy numbers from standard curves. LDR should cover at least 3 orders of magnitude, ideally 5-6 orders. Precision refers to intra-assay variation and is defined as standard deviation (SD) of technical replicates³⁰.

Amplicon purification and sequencing. Amplicons of all candidate reference genes were visualized in 1.5% agarose gels and bands were cut and purified using a QIAquick Gel Extraction Kit (#28506, Qiagen). Purified amplicons were subsequently sequenced using the Eurofins TubeSeq platform.

Stability analyses of reference gene candidates. To investigate the expression stability of the four reference gene candidates, two statistical algorithms were used: BestKeeper³³ and NormFinder³⁵. In brief, for BestKeeper, raw Ct values without any normalization are subjected to the calculation and the parameters of interest are SD (std dev [± CP]) and the Pearson coefficient of correlation (r). NormFinder utilizes normalized Ct values ($2^{-\Delta\text{Ct}}$) and can separately calculate the stability under each condition (IFN-I treatment, temperature) or total stability.

Statistical analysis

Statistical analysis was performed with GraphPad Prism 8 (GraphPad Software Inc., USA). To determine statistical significance among investigated groups, one-way analysis of variance (ANOVA) with Holm-Šidák's post-hoc test was performed. A two-tailed P value of <0.05 was considered to be significant.

Results

Performance of PCR primers targeting reference gene candidates

To evaluate the performance of the qRT-PCR assay, we first examined the specificity of the primer pairs with melting curve analysis, agarose gel electrophoresis and sequencing. Melting curve analysis revealed single peaks for all primer pairs (**Figure S1**). Agarose gel electrophoresis further demonstrated single bands of all the PCR products with the predicted sizes, indicating high specificity of all primer pairs (**Figure S1**). PCR products were sequenced and the specificity of the primers was confirmed (**Figure S2**). To evaluate the amplification efficiency, standard curves with 10-fold dilution steps were generated (**Figure S3**) and subsequently the linear dynamic range (LDR) and precision of each primer pair were assessed following the MIQE guideline³⁰. Amplification efficiencies of all tested primers met the validation criteria, notably 100.51% for *ACTB*, 99.53% for *EEF1A1*, 106.52% for *GAPDH* and 106.44% for *PGK1* (**Table 1**). The correlation coefficient (R^2) of all candidates is above 0.99, suggesting excellent linearity of the standard curves. The LDR values of all primers were in the range of 3 to 300,000 copies and precision values varied from 0.31 (*EEF1A1*) to 1.27 (*ACTB*) (**Table 1**). Thus, all the primers for reference gene candidates demonstrated satisfactory specificity and efficiency in qRT-PCR.

Expression profile of reference gene candidates in various tissues from *R. aegyptiacus*

To investigate the expression of reference gene candidates in tissues from *R. aegyptiacus*, qRT-PCR was performed with pooled cDNA from nose (nasal epithelium), trachea, lung, blood, spleen and duodenum. Threshold cycle (Ct) values were employed to determine the expression levels of the candidate reference genes. Their expression levels varied and *EEF1A1* displayed the highest expression levels across different tissues as indicated by the lowest Ct values. The overall Ct values of *EEF1A1*, *ACTB*, *GAPDH* and *PGK1* were 23 ± 1.5 , 33 ± 3 , 27 ± 2 and 27 ± 1.5 , respectively (Fig. 1). *EEF1A1* and *PGK1* showed the lowest variability in Ct values, suggesting that these two genes display the most stable expression across diverse tissues from *R. aegyptiacus*.

Table 1. Summary of the performance of primers employed in this study

Gene symbol	Efficiency [%]	Slope	LDR (copies)	Precision (SD of intra-assays)	Correlation coefficients (R^2)
<i>ACTB</i>	100.51	-3.3097	3-300,000	1.27	0.9999
<i>EEF1A1</i>	99.53	-3.3333	3-300,000	0.31	0.9969
<i>GAPDH</i>	106.52	-3.175	3-300,000	0.66	0.9991
<i>PGK1</i>	106.44	-3.1767	3-300,000	0.32	0.9976

Expression of candidate reference genes in primary bat fibroblasts upon IFN-I stimulation and incubation at variable temperatures

To investigate the expression stability of candidate reference genes, bat primary fibroblasts were incubated at 37°C or 40°C in the presence or absence of universal type I interferon (uIFN) for 4 h. We employed 37°C and 40°C to mimic the physiological daily oscillation of body temperature in bats⁹. The

expression levels of all candidate reference genes under these conditions were assessed by qRT-PCR. Ct values of *ACTB* showed a broad variety in Ct values from 29.7 to 39.01 at 40°C, indicating its unstable expression at higher temperature (Fig. 2). Compared to *ACTB*, the expression levels of *EEF1A1*, *GAPDH* and *PGK1* were relatively stable at 40°C, with Ct values of 22.3 ± 0.6 , 27.9 ± 1.5 and 28.8 ± 0.9 , respectively. Further, the expression levels of *EEF1A1*, *GAPDH* or *PGK1* were comparable at 37°C and 40°C, demonstrating stable expression of these potential reference genes under temperature oscillations. Since uIFN activates IFN-I pathway in bats³¹, we employed this cytokine to further investigate the expression of the candidate reference genes upon IFN-I stimulation. The mean Ct values of *GAPDH* decreased upon IFN-I stimulation at both 37°C and 40°C, indicating increased expression of *GAPDH* by IFN-I. The Ct values of *EEF1A1* and *PGK1* remained unchanged following stimulation with IFN-I stimulation at either 37°C or 40°C, suggesting their stable expression under these experimental conditions (Fig. 2). We therefore conclude that expression stabilities of *ACTB* and *GAPDH* are impaired by high temperature and IFN-I, respectively.

Expression stability analysis of reference gene candidates under different conditions

To quantitatively evaluate the expression stability of candidate reference genes, qPCR results were analysed with the statistical algorithms BestKeeper and NormFinder. BestKeeper enables pairwise correlation, regression analysis^{32,33} and calculations of standard deviation (SD) of all Ct values [SD (\pm Ct)] and the standard deviation of absolute regulation coefficients [SD (\pm x-fold)] as indicators of expression variability. A suitable reference gene should display values of < 1 for SD (\pm Ct) and < 2 for SD (\pm x-fold), as well as 1 for coefficient of correlation (r)³⁴. According to this algorithm, the [SD (\pm Ct)] values for *ACTB*, *EEF1A1*, *GAPDH* and *PGK1* were 1.27, 0.31, 0.66 and 0.32, along with their corresponding r values of 0.64, 0.95, 0.65 and 0.84. Thus, expression stability for candidate reference genes ranks as following: *EEF1A1*, *PGK1*, *GAPDH*, and *ACTB* (**Table 2**).

NormFinder was employed as the second algorithm to determine gene stability, since it allows evaluation of the overall stability as well as the individual stability for each condition³⁵. The most stable reference genes display stability values close to 0 according to this algorithm. Based on this method, we calculated the overall and individual stability values accordingly. The total stability values for *ACTB*, *EEF1A1*, *GAPDH* and *PGK1* were 0.096, 0.015, 0.053 and 0.017, respectively, suggesting *EEF1A1* as the most stable reference gene combining all conditions. *EEF1A1* also displayed the highest expression stability under high temperature or upon IFN-I treatment (**Table 3**). Altogether, both algorithms demonstrate that *EEF1A1* is the reference gene with the highest expression stability, followed by *PGK1*, *GAPDH*, whereas *ACTB* has the lowest stability.

Table 2. Stability analysis of reference gene candidates with BestKeeper.

Parameters	Reference gene			
	<i>ACTB</i>	<i>EEF1A1</i>	<i>GAPDH</i>	<i>PGK1</i>
BestKeeper				
geo Mean [CP]	32,57	22,38	27,97	28,81
ar Mean [CP]	32,60	22,38	27,98	28,81
min [CP]	29,74	21,96	26,70	28,24
max [CP]	34,30	23,07	29,08	29,68
std dev [± CP]	1,27	0,31	0,66	0,32
CV [% CP]	3,91	1,42	2,37	1,03
min [x-fold]	-7,11	-1,33	-2,42	-1,49
max [x-fold]	3,31	1,62	2,16	1,82
std dev [± x-fold]	2,42	1,25	1,58	1,23
coeff. of corr. [r]	0,64	0,95	0,65	0,84
p-value	0,01	0,00	0,01	0,00

Table 3. Stability analysis of reference gene candidates with NormFinder.

Norm Finder	Stability in various conditions		
	<i>total</i>	<i>uIFN</i>	<i>Temperature</i>
<i>EEF1A1</i>	0,015	0,016	0,015
<i>PGK1</i>	0,017	0,018	0,017
<i>GAPDH</i>	0,053	0,079	0,045
<i>ACTB</i>	0,096	0,082	0,140

GAPDH expression is induced by IFN-I in *R. aegyptiacus* cells

To evaluate the relative expression levels of *ACTB*, *GAPDH* and *PGK1* under different conditions, we normalized each candidate to the most stable reference gene, *EEF1A1* (Fig. 3A, **B**). The relative expression levels of *PGK1* remained stable at 37°C and 40°C irrespective of the IFN-I treatment. *ACTB* expression was also stable at 37°C in the presence of IFN-I. However, the expression level was significantly reduced following a 2 h IFN-I stimulation at 40°C (Fig. 3B). Intriguingly, the expression of *GAPDH* was significantly increased in cells treated with IFN-I at 37°C and 40°C, suggesting that the induction of *GAPDH* by IFN-I is temperature independent in *R. aegyptiacus* (Fig. 3A, **B**). To investigate whether *GAPDH* induction by IFN-I is specific to *R. aegyptiacus*, we stimulated human fibroblasts with IFN-I at 37°C and 40°C (Fig. 3C, **D**). Both human *GAPDH* and *ACTB* have been previously used as reference genes in several qRT-PCR studies^{36,37}. Indeed, both genes displayed good expression stability at 37°C, yet the variation of Ct values

at 40°C argued against stability of human *GAPDH* and *ACTB* at 40°C. The relative expression of human *GAPDH* normalized against *ACTB* remained unchanged upon IFN-I treatment either at 37°C or 40°C, revealing that human *GAPDH* expression in fibroblasts is not modulated by IFN-I (Fig. 3C, D). Overall, we conclude that IFN-I triggers *GAPDH* expression specifically in *R. aegyptiacus*.

Discussion

It is of particular interest to study the unique immune system of bats, since bats have been identified as the reservoirs for multiple highly pathogenic viruses. Accurate gene transcription measurements require selection of genes that maintain high stability under various experimental conditions. In this study, we evaluated the suitability of the widely used reference genes and ultimately validated *EEF1A1* as the most stable reference gene in *R. aegyptiacus* under conditions relevant for the biology of this species^{36,38-41}. The choice for *ACTB*, *GAPDH*, *PGK1* and *EEF1A1* was supported by their stable expression in several other species^{14,32,36,39,42-48}. As bats display unique physiological features, such as oscillation of body temperature²⁴ and constitutive IFN-I expression in some species¹⁰, we have evaluated the expression of selected reference genes in different tissues and cells from *R. aegyptiacus* under various temperatures with or without IFN-I stimulation *in vitro*. By normalizing the qRT-PCR data to *EEF1A1*, we revealed that the expression of *GAPDH* was significantly induced by IFN-I, excluding the use of this commonly used reference gene in *R. aegyptiacus*. Consistent with our study, many reports have also demonstrated that the expression of *GAPDH* and *ACTB* was unstable in various tissues of mice and humans, cell types or under certain conditions^{37,49-52}. Whether *GAPDH* expression is induced by IFN-I, and whether *GAPDH* and *ACTB* are suitable reference genes in other bat species, require further investigations.

Our finding that the expression of *GAPDH*, one of the key enzymes in glycolysis, is induced by IFN-I in *R. aegyptiacus* may have implications for the immunometabolism of bats. It is well established that metabolic reprogramming in cells controls their immune responses^{53,54}. Glycolysis is commonly utilized by various immune cells to enable prompt responses to infections. In bone marrow derived macrophages, aerobic glycolysis promotes IL-1 β production upon LPS stimulation or *Bordetella pertussis* infection⁵⁵. In CD4⁺ and CD8⁺ T-cells⁵⁶⁻⁶⁰, as well as in NK cells^{61,62}, glycolysis is required for their effector functions, such as IFN γ production and cytotoxicity. In human plasmacytoid dendritic cells (pDCs) and monocyte-derived DCs (moDC), glycolysis promotes IFN-I production upon TLR9 or RIG-I activation, respectively⁶³. Further, IFN-I induces a metabolic shift towards glycolysis, contributing to the antiviral activity in fibroblasts and antigen presentation in DCs^{64,65}. On the other hand, lactate, the end metabolite of glycolysis, directly binds to mitochondrial antiviral-signaling protein (MAVS), and consequently inhibits its activation and IFN-I production⁶⁶. Thus, outcomes of such metabolic shift vary in diverse cells or under different stimulations. It has been speculated that the nectarivore bat *Glossophaga soricina* employs high rates of glycolysis to generate ATP during flight⁶⁷. As a fruit bat, *R. aegyptiacus* could directly utilize dietary sugars to fuel both roosting and flight metabolism⁶⁸. Whether induction of *GAPDH* expression in this species impacts on metabolic reprogramming towards glycolysis, needs to be clarified. Moreover,

whether and how such metabolism shift affects IFN-I signalling or other immune pathways in *R. aegyptiacus* remains to be uncovered.

In addition to being an essential component in glycolysis, *GAPDH* plays diverse roles in many other cellular processes, such as cell death, RNA export and cytoskeleton dynamics⁶⁹. Upon serum deprivation and DNA damage, *GAPDH* translocates to the mitochondria and interacts with voltage-dependent anion channel (VDAC), leading to apoptosis⁷⁰. It can also bind to the 3' untranslated region of *TNF α* mRNA and repress *TNF α* expression in human monocytes and macrophages⁷¹. Hence, *GAPDH* upregulation by IFN-I may contribute to apoptosis induction and *TNF α* repression in *R. aegyptiacus*, which could represent novel mechanisms of preventing excessive inflammation during viral infections. Undoubtedly, changes in cellular bioenergetic features, either in immune and/or virus permissive cells, alter their antimicrobial features which may impact on the host defense against pathogens.

Overall, our study provides an extensive stability analysis of reference genes by identifying *EEF1A1* as the most stable reference gene for accurate gene transcription studies in bats, particularly *R. aegyptiacus*. Our findings also open a new investigation avenue by showing that *GAPDH* is regulated by IFN-I. The role of bats in disease epidemics, which reach global scale, is increasingly recognized^{72–75}. Thus, robust and innovative research focusing on these reservoir hosts is currently a priority. In this line, *R. aegyptiacus*, representing one of the species that is most frequently used in infectiology research, needs to be thoroughly analysed. Defining rigorous standards for gene transcription studies assist the progress on virus-reservoir host interactions.

Declarations

Conflict of interest

No potential conflict of interest was stated by the authors.

Acknowledgements

We thank Dr. Donata Hoffmann and Nico Joel Halwe (Institute of Diagnostic Virology, Friedrich-Loeffler-Institut, Germany) for providing homogenized *R. aegyptiacus* tissue samples and Lisa Loerzer and Silke Rehbein for skilled technical assistance.

Author contributions

Data curation and data analysis: VF and GP; sample preparation: ABB, VF and GP; funding, study design and supervision: GP and AD; manuscript writing and editing: VF, ABB, AD, GP.

References

1. Irving, A. T., Ahn, M., Goh, G., Anderson, D. E. & Wang, L.-F. Lessons from the host defences of bats, a unique viral reservoir. *Nature* **589**, 363–370; 10.1038/s41586-020-03128-0 (2021).
2. Amman, B. R. *et al.* Oral shedding of Marburg virus in experimentally infected Egyptian fruit bats (*Rousettus aegyptiacus*). *Journal of wildlife diseases* **51**, 113–124; 10.7589/2014-08-198 (2015).
3. Kalunda, M. *et al.* Kasokero virus: a new human pathogen from bats (*Rousettus aegyptiacus*) in Uganda. *The American journal of tropical medicine and hygiene* **35**, 387–392; 10.4269/ajtmh.1986.35.387 (1986).
4. Amman, B. R. *et al.* A Recently Discovered Pathogenic Paramyxovirus, Sosuga Virus, is Present in *Rousettus aegyptiacus* Fruit Bats at Multiple Locations in Uganda. *Journal of wildlife diseases* **51**, 774–779; 10.7589/2015-02-044 (2015).
5. Schlottau, K. *et al.* SARS-CoV-2 in fruit bats, ferrets, pigs, and chickens: an experimental transmission study. *The Lancet. Microbe* **1**, e218-e225; 10.1016/S2666-5247(20)30089-6 (2020).
6. Balkema-Buschmann, A. *et al.* Productive Propagation of Rift Valley Fever Phlebovirus Vaccine Strain MP-12 in *Rousettus aegyptiacus* Fruit Bats. *Viruses* **10**; 10.3390/v10120681 (2018).
7. Paweska, J. T. *et al.* Experimental Inoculation of Egyptian Fruit Bats (*Rousettus aegyptiacus*) with Ebola Virus. *Viruses* **8**; 10.3390/v8020029 (2016).
8. Seifert, S. N. *et al.* *Rousettus aegyptiacus* Bats Do Not Support Productive Nipah Virus Replication. *The Journal of infectious diseases* **221**, S407-S413; 10.1093/infdis/jiz429 (2020).
9. Kulzer, E. Temperaturregulation bei Flughunden der Gattung *Rousettus* Gray. *Z. Vergl. Physiol.* **46**, 595–618; 10.1007/BF00298161 (1963).
10. Zhou, P. *et al.* Contraction of the type I IFN locus and unusual constitutive expression of IFN- α in bats. *Proceedings of the National Academy of Sciences of the United States of America* **113**, 2696–2701; 10.1073/pnas.1518240113 (2016).
11. Pavlovich, S. S. *et al.* The Egyptian Rousette Genome Reveals Unexpected Features of Bat Antiviral Immunity. *Cell* **173**, 1098-1110.e18; 10.1016/j.cell.2018.03.070 (2018).
12. Subudhi, S., Rapin, N. & Misra, V. Immune System Modulation and Viral Persistence in Bats: Understanding Viral Spillover. *Viruses* **11**; 10.3390/v11020192 (2019).
13. Banerjee, A., Rapin, N., Bollinger, T. & Misra, V. Lack of inflammatory gene expression in bats: a unique role for a transcription repressor. *Scientific reports* **7**, 2232; 10.1038/s41598-017-01513-w (2017).
14. Ahn, M. *et al.* Dampened NLRP3-mediated inflammation in bats and implications for a special viral reservoir host. *Nature microbiology* **4**, 789–799; 10.1038/s41564-019-0371-3 (2019).

15. Guito, J. C. *et al.* Asymptomatic Infection of Marburg Virus Reservoir Bats Is Explained by a Strategy of Immunoprotective Disease Tolerance. *Current biology : CB* **31**, 257-270.e5; 10.1016/j.cub.2020.10.015 (2021).
16. Wang, L.-F., Gamage, A. M., Chan, W. O. Y., Hiller, M. & Teeling, E. C. Decoding bat immunity: the need for a coordinated research approach. *Nature reviews. Immunology*, 10.1038/s41577-021-00523-0 (2021).
17. Gamage, A. M. *et al.* Immunophenotyping monocytes, macrophages and granulocytes in the Pteropodid bat *Eonycteris spelaea*. *Scientific reports* **10**, 309; 10.1038/s41598-019-57212-1. (2020).
18. Martínez Gómez, J. M. *et al.* Phenotypic and functional characterization of the major lymphocyte populations in the fruit-eating bat *Pteropus alecto*. *Scientific reports* **6**, 37796; 10.1038/srep37796 (2016).
19. Periasamy, P. *et al.* Studies on B Cells in the Fruit-Eating Black Flying Fox (*Pteropus alecto*). *Frontiers in immunology* **10**, 489; 10.3389/fimmu.2019.00489 (2019).
20. Petriccione, M., Mastrobuoni, F., Zampella, L. & Scortichini, M. Reference gene selection for normalization of RT-qPCR gene expression data from *Actinidia deliciosa* leaves infected with *Pseudomonas syringae* pv. *actinidiae*. *Scientific reports* **5**, 16961; 10.1038/srep16961 (2015).
21. McMillan, M. & Pereg, L. Evaluation of reference genes for gene expression analysis using quantitative RT-PCR in *Azospirillum brasilense*. *PloS one* **9**, e98162; 10.1371/journal.pone.0098162 (2014).
22. Radonić, A. *et al.* Guideline to reference gene selection for quantitative real-time PCR. *Biochemical and biophysical research communications* **313**, 856–862; 10.1016/j.bbrc.2003.11.177 (2004).
23. Cruz-Neto, A. P., Garland, T. & Abe, A. S. Diet, phylogeny, and basal metabolic rate in phyllostomid bats. *Zoology (Jena, Germany)* **104**, 49–58; 10.1078/0944-2006-00006 (2001).
24. HOCK, R. J. THE METABOLIC RATES AND BODY TEMPERATURES OF BATS. *The Biological Bulletin* **101**, 289–299; 10.2307/1538547 (1951).
25. O'Mara, M. T. *et al.* Cyclic bouts of extreme bradycardia counteract the high metabolism of frugivorous bats. *eLife* **6**; 10.7554/eLife.26686 (2017).
26. Noll, U. G. Body temperature, oxygen consumption, noradrenaline response and cardiovascular adaptations in the flying fox, *Rousettus aegyptiacus*. *Comparative Biochemistry and Physiology Part A: Physiology* **63**, 79–88; 10.1016/0300-9629(79)90631-5 (1979).
27. Brook, C. E. *et al.* Accelerated viral dynamics in bat cell lines, with implications for zoonotic emergence. *eLife* **9**; 10.7554/eLife.48401 (2020).

28. Koh, J. *et al.* ABCB1 protects bat cells from DNA damage induced by genotoxic compounds. *Nature communications* **10**, 2820; 10.1038/s41467-019-10495-4 (2019).
29. Xie, J. *et al.* Dampened STING-Dependent Interferon Activation in Bats. *Cell host & microbe* **23**, 297-301.e4; 10.1016/j.chom.2018.01.006 (2018).
30. Bustin, S. A. *et al.* The MIQE guidelines: minimum information for publication of quantitative real-time PCR experiments. *Clinical chemistry* **55**, 611–622; 10.1373/clinchem.2008.112797 (2009).
31. La Cruz-Rivera, P. C. de *et al.* The IFN Response in Bats Displays Distinctive IFN-Stimulated Gene Expression Kinetics with Atypical RNASEL Induction. *Journal of immunology (Baltimore, Md. : 1950)* **200**, 209–217; 10.4049/jimmunol.1701214 (2018).
32. Klie, M. & Debener, T. Identification of superior reference genes for data normalisation of expression studies via quantitative PCR in hybrid roses (*Rosa hybrida*). *BMC research notes* **4**, 518; 10.1186/1756-0500-4-518 (2011).
33. Pfaffl, M. W., Tichopad, A., Prgomet, C. & Neuvians, T. P. Determination of stable housekeeping genes, differentially regulated target genes and sample integrity: BestKeeper–Excel-based tool using pair-wise correlations. *Biotechnology letters* **26**, 509–515; 10.1023/b:bile.0000019559.84305.47. (2004).
34. Pombo, M. A., Zheng, Y., Fei, Z., Martin, G. B. & Rosli, H. G. Use of RNA-seq data to identify and validate RT-qPCR reference genes for studying the tomato-Pseudomonas pathosystem. *Scientific reports* **7**, 44905; 10.1038/srep44905 (2017).
35. Andersen, C. L., Jensen, J. L. & Ørntoft, T. F. Normalization of real-time quantitative reverse transcription-PCR data: a model-based variance estimation approach to identify genes suited for normalization, applied to bladder and colon cancer data sets. *Cancer research* **64**, 5245–5250; 10.1158/0008-5472.CAN-04-0496 (2004).
36. Dheda, K. *et al.* Validation of housekeeping genes for normalizing RNA expression in real-time PCR. *BioTechniques* **37**, 112-4, 116, 118-9; 10.2144/04371RR03 (2004).
37. Glare, E. M., Divjak, M., Bailey, M. J. & Walters, E. H. beta-Actin and GAPDH housekeeping gene expression in asthmatic airways is variable and not suitable for normalising mRNA levels. *Thorax* **57**, 765–770; 10.1136/thorax.57.9.765 (2002).
38. Suzuki, T., Higgins, P. J. & Crawford, D. R. Control selection for RNA quantitation. *BioTechniques* **29**, 332–337; 10.2144/00292rv02 (2000).
39. Falkenberg, V. R., Whistler, T., Murray, J. R., Unger, E. R. & Rajeevan, M. S. Identification of Phosphoglycerate Kinase 1 (PGK1) as a reference gene for quantitative gene expression measurements in human blood RNA. *BMC research notes* **4**, 324; 10.1186/1756-0500-4-324 (2011).

40. Molina, C. E. *et al.* Identification of optimal reference genes for transcriptomic analyses in normal and diseased human heart. *Cardiovascular research* **114**, 247–258; 10.1093/cvr/cvx182 (2018).
41. Sarwar, M. B. *et al.* Identification and validation of superior housekeeping gene(s) for qRT-PCR data normalization in *Agave sisalana* (a CAM-plant) under abiotic stresses. *Physiology and molecular biology of plants : an international journal of functional plant biology* **26**, 567–584; 10.1007/s12298-020-00760-y (2020).
42. Aminfar, Z., Rabiei, B., Tohidfar, M. & Mirjalili, M. H. Selection and validation of reference genes for quantitative real-time PCR in *Rosmarinus officinalis* L. in various tissues and under elicitation. *Biocatalysis and Agricultural Biotechnology* **20**, 101246; 10.1016/j.bcab.2019.101246 (2019).
43. Bai, B., Ren, J., Bai, F. & Hao, L. Selection and validation of reference genes for gene expression studies in *Pseudomonas brassicacearum* GS20 using real-time quantitative reverse transcription PCR. *PloS one* **15**, e0227927; 10.1371/journal.pone.0227927 (2020).
44. Ham, S., Harrison, C., Southwick, G. & Temple-Smith, P. Selection of internal control genes for analysis of gene expression in normal and diseased human dermal fibroblasts using quantitative real-time PCR. *Experimental dermatology* **25**, 911–914; 10.1111/exd.13091 (2016).
45. Huggett, J., Dheda, K., Bustin, S. & Zumla, A. Real-time RT-PCR normalisation; strategies and considerations. *Genes and immunity* **6**, 279–284; 10.1038/sj.gene.6364190 (2005).
46. Panina, Y., Germond, A., Masui, S. & Watanabe, T. M. Validation of Common Housekeeping Genes as Reference for qPCR Gene Expression Analysis During iPS Reprogramming Process. *Scientific reports* **8**, 8716; 10.1038/s41598-018-26707-8 (2018).
47. Sullivan-Gunn, M., Hinch, E., Vaughan, V. & Lewandowski, P. Choosing a stable housekeeping gene and protein is essential in generating valid gene and protein expression results. *British journal of cancer* **104**, 1055; author reply 1056; 10.1038/bjc.2011.35 (2011).
48. Fujii, H. *et al.* Functional analysis of *Rousettus aegyptiacus* "signal transducer and activator of transcription 1" (STAT1). *Developmental and comparative immunology* **34**, 598–602; 10.1016/j.dci.2010.01.004 (2010).
49. Sabath, D. E., Broome, H. & Prystowsky, M. B. Glyceraldehyde-3-phosphate dehydrogenase mRNA is a major interleukin 2-induced transcript in a cloned T-helper lymphocyte. *Gene* **91**, 185–191; 10.1016/0378-1119(90)90087-8 (1990).
50. Graven, K. K., McDonald, R. J. & Farber, H. W. Hypoxic regulation of endothelial glyceraldehyde-3-phosphate dehydrogenase. *The American journal of physiology* **274**, C347-55; 10.1152/ajpcell.1998.274.2.C347 (1998).

51. Hazell, A. S., Desjardins, P. & Butterworth, R. F. Increased expression of glyceraldehyde-3-phosphate dehydrogenase in cultured astrocytes following exposure to manganese. *Neurochemistry International* **35**, 11–17; 10.1016/s0197-0186(99)00024-8 (1999).
52. Nakayama, T. *et al.* Assessment of suitable reference genes for RT-qPCR studies in chronic rhinosinusitis. *Scientific reports* **8**, 1568; 10.1038/s41598-018-19834-9 (2018).
53. O'Neill, L. A. J., Kishton, R. J. & Rathmell, J. A guide to immunometabolism for immunologists. *Nature reviews. Immunology* **16**, 553–565; 10.1038/nri.2016.70 (2016).
54. O'Neill, L. A. J. & Pearce, E. J. Immunometabolism governs dendritic cell and macrophage function. *The Journal of experimental medicine* **213**, 15–23; 10.1084/jem.20151570 (2016).
55. Tannahill, G. M. *et al.* Succinate is an inflammatory signal that induces IL-1 β through HIF-1 α . *Nature* **496**, 238–242; 10.1038/nature11986 (2013).
56. Cham, C. M., Driessens, G., O'Keefe, J. P. & Gajewski, T. F. Glucose deprivation inhibits multiple key gene expression events and effector functions in CD8+ T cells. *European journal of immunology* **38**, 2438–2450; 10.1002/eji.200838289 (2008).
57. Cham, C. M. & Gajewski, T. F. Glucose availability regulates IFN-gamma production and p70S6 kinase activation in CD8+ effector T cells. *Journal of immunology (Baltimore, Md. : 1950)* **174**, 4670–4677; 10.4049/jimmunol.174.8.4670 (2005).
58. Chang, C.-H. *et al.* Posttranscriptional control of T cell effector function by aerobic glycolysis. *Cell* **153**, 1239–1251; 10.1016/j.cell.2013.05.016 (2013).
59. Macintyre, A. N. *et al.* The glucose transporter Glut1 is selectively essential for CD4 T cell activation and effector function. *Cell metabolism* **20**, 61–72; 10.1016/j.cmet.2014.05.004 (2014).
60. Gerriets, V. A. *et al.* Metabolic programming and PDHK1 control CD4+ T cell subsets and inflammation. *The Journal of clinical investigation* **125**, 194–207; 10.1172/JCI76012 (2015).
61. Keating, S. E. *et al.* Metabolic Reprogramming Supports IFN- γ Production by CD56bright NK Cells. *Journal of immunology (Baltimore, Md. : 1950)* **196**, 2552–2560; 10.4049/jimmunol.1501783 (2016).
62. Mah, A. Y. *et al.* Glycolytic requirement for NK cell cytotoxicity and cytomegalovirus control. *JCI insight* **2**; 10.1172/jci.insight.95128 (2017).
63. Fekete, T. *et al.* Human Plasmacytoid and Monocyte-Derived Dendritic Cells Display Distinct Metabolic Profile Upon RIG-I Activation. *Frontiers in immunology* **9**, 3070; 10.3389/fimmu.2018.03070 (2018).
64. Burke, J. D., Platanias, L. C. & Fish, E. N. Beta interferon regulation of glucose metabolism is PI3K/Akt dependent and important for antiviral activity against coxsackievirus B3. *Journal of virology* **88**, 3485–

3495; 10.1128/JVI.02649-13 (2014).

65. Pantel, A. *et al.* Direct type I IFN but not MDA5/TLR3 activation of dendritic cells is required for maturation and metabolic shift to glycolysis after poly IC stimulation. *PLoS biology* **12**, e1001759; 10.1371/journal.pbio.1001759 (2014).

66. Zhang, W. *et al.* Lactate Is a Natural Suppressor of RLR Signaling by Targeting MAVS. *Cell* **178**, 176–189.e15; 10.1016/j.cell.2019.05.003 (2019).

67. Kelm, D. H., Simon, R., Kuhlow, D., Voigt, C. C. & Ristow, M. High activity enables life on a high-sugar diet: blood glucose regulation in nectar-feeding bats. *Proceedings. Biological sciences* **278**, 3490–3496; 10.1098/rspb.2011.0465 (2011).

68. Amitai, O. *et al.* Fruit bats (Pteropodidae) fuel their metabolism rapidly and directly with exogenous sugars. *The Journal of experimental biology* **213**, 2693–2699; 10.1242/jeb.043505 (2010).

69. Tristan, C., Shahani, N., Sedlak, T. W. & Sawa, A. The diverse functions of GAPDH: views from different subcellular compartments. *Cellular signalling* **23**, 317–323; 10.1016/j.cellsig.2010.08.003 (2011).

70. Tarze, A. *et al.* GAPDH, a novel regulator of the pro-apoptotic mitochondrial membrane permeabilization. *Oncogene* **26**, 2606–2620; 10.1038/sj.onc.1210074 (2007).

71. Millet, P., Vachharajani, V., McPhail, L., Yoza, B. & McCall, C. E. GAPDH Binding to TNF- α mRNA Contributes to Posttranscriptional Repression in Monocytes: A Novel Mechanism of Communication between Inflammation and Metabolism. *Journal of immunology (Baltimore, Md. : 1950)* **196**, 2541–2551; 10.4049/jimmunol.1501345 (2016).

72. Frick, W. F., Kingston, T. & Flanders, J. A review of the major threats and challenges to global bat conservation. *Annals of the New York Academy of Sciences* **1469**, 5–25; 10.1111/nyas.14045 (2020).

73. Gorbunova, V., Seluanov, A. & Kennedy, B. K. The World Goes Bats: Living Longer and Tolerating Viruses. *Cell metabolism* **32**, 31–43; 10.1016/j.cmet.2020.06.013 (2020).

74. Luis, A. D. *et al.* A comparison of bats and rodents as reservoirs of zoonotic viruses: are bats special? *Proceedings. Biological sciences* **280**, 20122753; 10.1098/rspb.2012.2753 (2013).

75. Turmelle, A. S. & Olival, K. J. Correlates of viral richness in bats (order Chiroptera). *EcoHealth* **6**, 522–539; 10.1007/s10393-009-0263-8 (2009).

76. Halwe, N. J. *et al.* Egyptian Fruit Bats (*Rousettus aegyptiacus*) Were Resistant to Experimental Inoculation with Avian-Origin Influenza A Virus of Subtype H9N2, But Are Susceptible to Experimental Infection with Bat-Borne H9N2 Virus. *Viruses* **13**; 10.3390/v13040672 (2021).

77. Chomczynski, P. & Sacchi, N. Single-step method of RNA isolation by acid guanidinium thiocyanate-phenol-chloroform extraction. *Analytical biochemistry* **162**, 156–159; 10.1006/abio.1987.9999 (1987).
78. Lee, C., Kim, J., Shin, S. G. & Hwang, S. Absolute and relative QPCR quantification of plasmid copy number in *Escherichia coli*. *Journal of biotechnology* **123**, 273–280; 10.1016/j.jbiotec.2005.11.014 (2006).

Figures

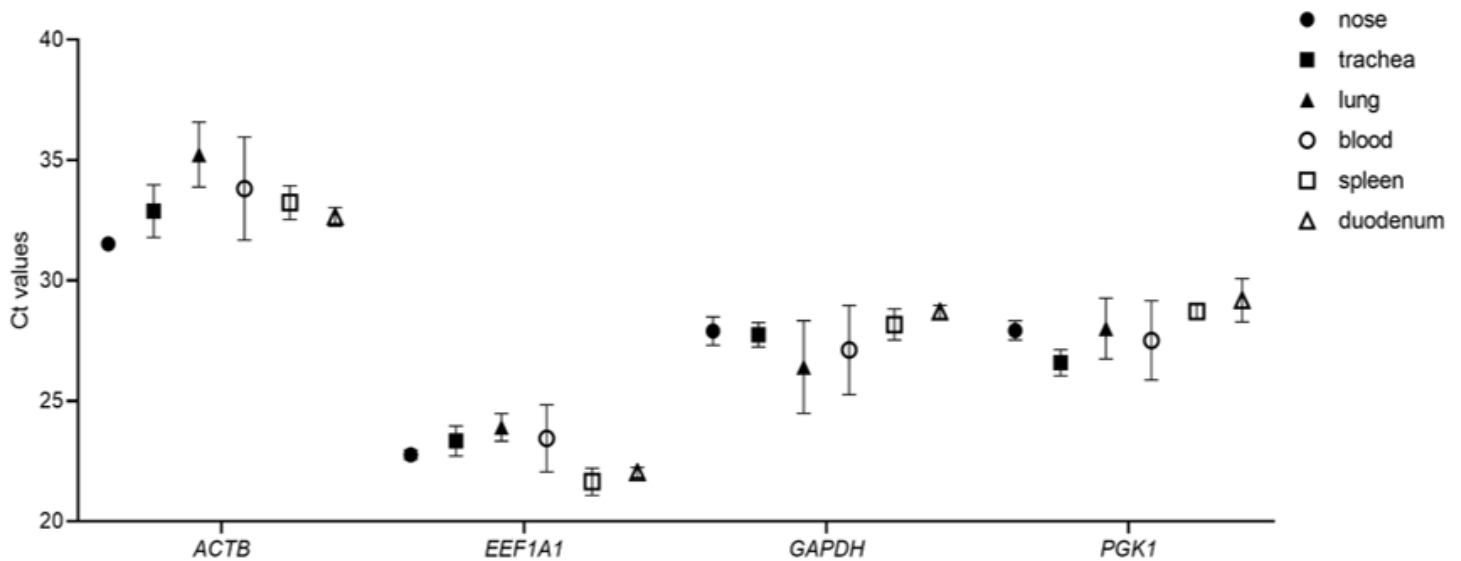


Figure 1

Ct values of selected reference genes in various tissues from *Rousettus aegyptiacus*. RNA was extracted from nose, trachea, lung, blood, spleen and duodenum from 12 animals. Expression of reference gene candidates were determined via qRT-PCR. Data show mean \pm SD from 3 independent experiments.

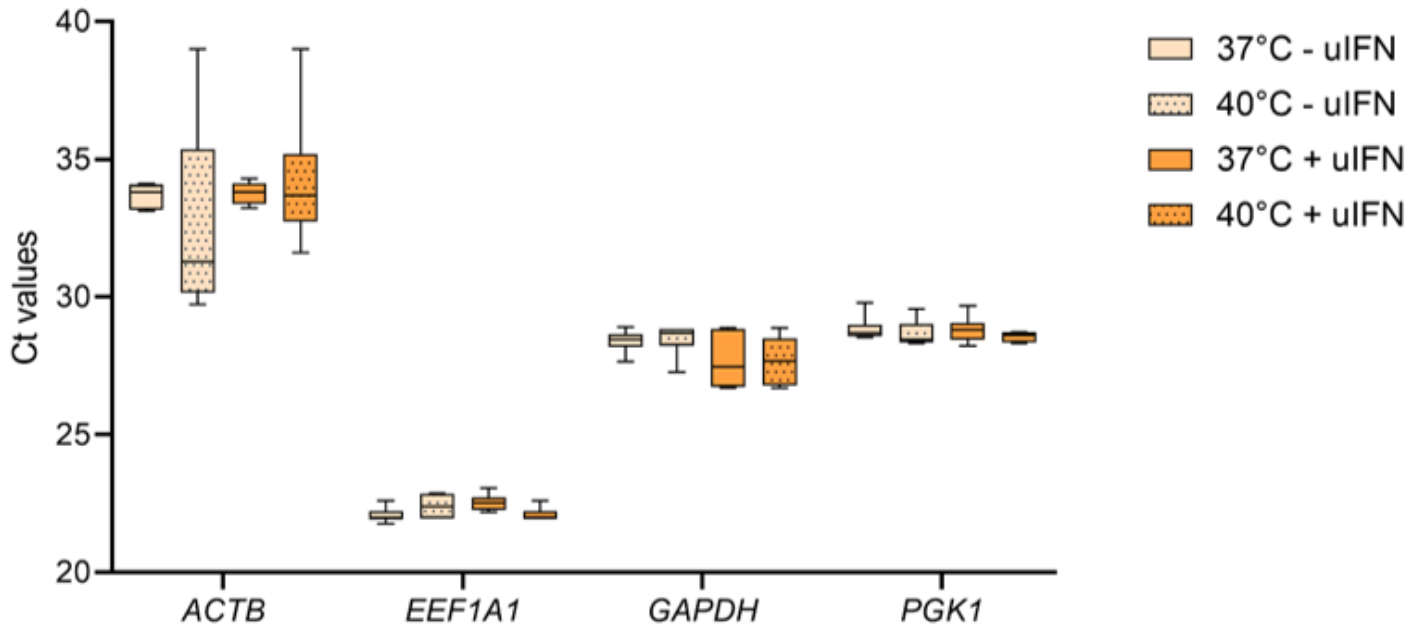


Figure 2

Expression stability of candidate reference genes under different conditions. Bat primary fibroblasts were incubated at 37°C or 40°C in the presence or absence of 1000U/ml universal type I interferon (uIFN). Gene expression levels of ACTB, EEF1A1, GAPDH and PGK1 were determined with qRT-PCR. Data show mean±SD from 3 independent experiments.

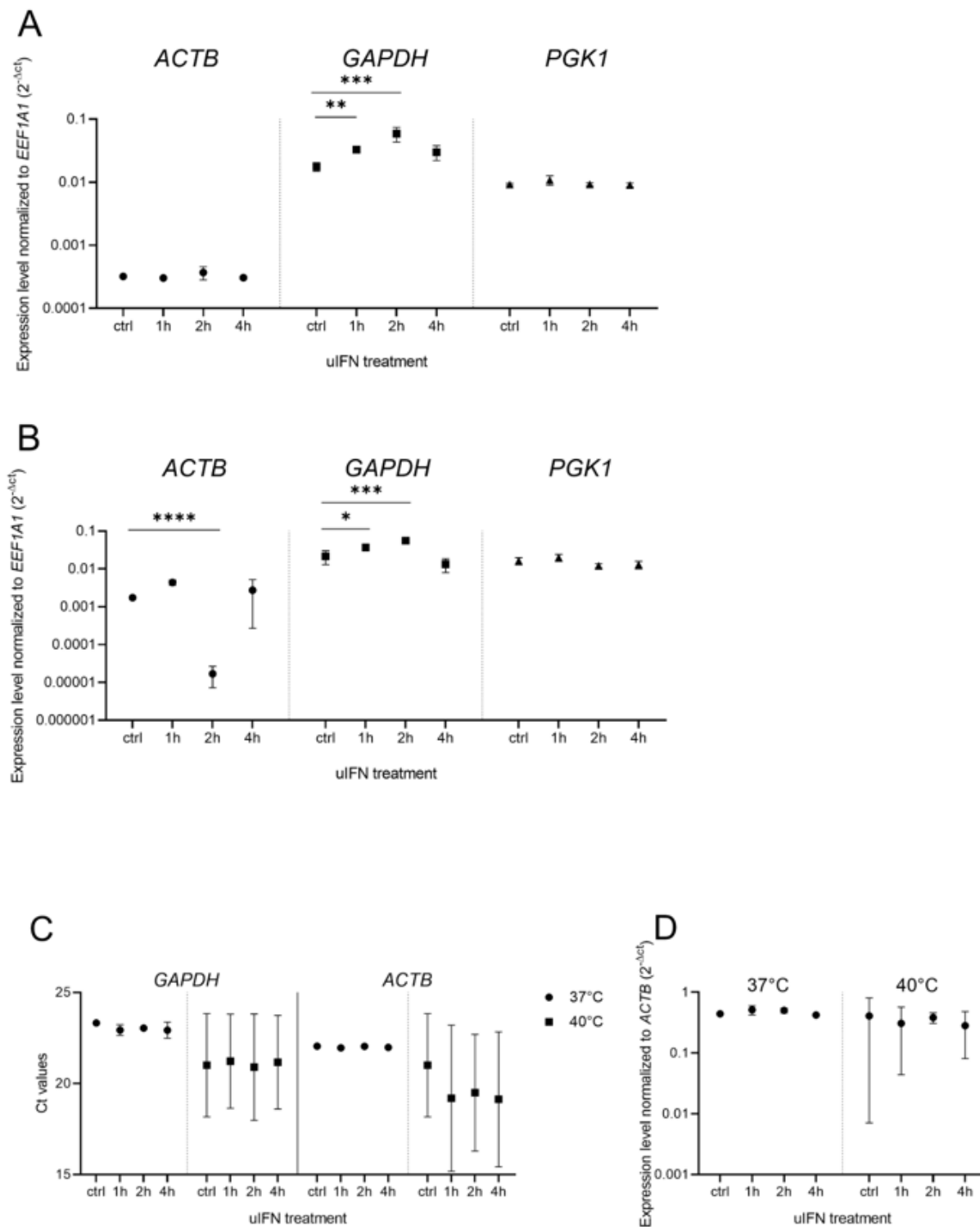


Figure 3

GAPDH expression is induced by IFN-I in *R. aegyptiacus*. (A, B) Relative gene expression of *ACTB*, *GAPDH* and *PGK1* normalized to *EEF1A1* upon uIFN treatment at 37°C (A) or 40°C (B). (C, D) Ct values of human *ACTB* and *GAPDH* (C) and relative expression of human *GAPDH* normalized to *ACTB* (D) in human fibroblasts upon uIFN treatment and incubation at 37°C or 40°C. Bat (A, B) or human (C, D) primary fibroblasts were stimulated with PBS (ctrl) or 1000U/ml universal type I interferon (uIFN) for indicated

time at 37°C or 40°C. Gene expression levels of ACTB, GAPDH and PGK1 were determined with qRT-PCR. Data show mean±SD from 3 independent experiments. The statistical significance was calculated using one-way ANOVA with Holm-Šidák's post-hoc test. (*) $p \leq 0.05$, (***) $p \leq 0.001$, (****) $p \leq 0.0001$.

Supplementary Files

This is a list of supplementary files associated with this preprint. Click to download.

- [Supplementaryfigures.docx](#)